

Change in the type of bifurcation resulting in periodic oscillations in delayed feedback diode lasers

A.P. Napartovich, A.G. Sukharev

Abstract. The appearance of oscillating regimes in a delayed feedback diode laser is studied analytically and numerically. Based on the Lang–Kobayashi model, the transition of the usual oscillation mechanism, related to the transition through the Hopf bifurcation, to hard excitation of the spike regime is studied. The change in the regime of the instability development has a nature of a phase transition. An explicit expression is derived for the frequency of small harmonic oscillations appearing during the transition through the Andronov–Hopf bifurcation. The boundary between two different regimes of the development of laser power oscillations is determined in the parameter space.

Keywords: diode laser, generation dynamics, delayed feedback, bifurcation.

1. Introduction

A delayed feedback diode laser is widely used in quantum electronics due to many dynamic operation regimes [1]. The variety of its dynamic regimes is caused by the presence of two coupled resonators, one of which is formed by semiconductor crystal facets and the other – by a highly reflecting end-face and an external mirror. The modern theory of dynamics of delayed feedback laser diodes is based on Lang–Kobayashi (LK) equations [2]. In the LK approximation, the reflection of radiation incident from the external mirror on the diode facets is neglected. The foundations of the theory of external feedback diode lasers are presented in book [1]. A great number of parameters entering LK equations strongly complicate the classification of regimes of generation dynamics.

Particular solutions of the system of LK equations, the so-called stationary states in which the radiation intensity is independent of time, can be easily found. The change in the field phase in the stationary state is characterised by the stationary frequency Ω . The linearisation of LK equations with respect to the stationary states and the search for the solution, which exponentially depends on time $[(\exp(\lambda t))$,

lead to the transcendental expression for exponent factors λ [1, 3]. The transcendence of the characteristic equation of the linear perturbation theory is related to the delay of the signal reflected from the external mirror. This equation involves five physical parameters, which complicates the general analysis of appearing instabilities. The number of roots of the transcendent equation, generally speaking, is not limited. In the general case, the roots are complex. The positive real part of the eigenvalue means the instability of the stationary solution (stationary state). The stationary state instability can develop due to the aperiodic increase in perturbations: such instabilities develop in bifurcations of the saddle–node type [4]. In this case, the system undergoes a transition to another stable state due to the instability development. The stationary state instability with respect to the appearance of harmonic oscillations at the Hopf bifurcation point is of special interest because a couple of solutions with the zero real part appear at this point in the transcendent equation. This means that upon passing through the Hopf bifurcation, undamped harmonic oscillations appear whose amplitude smoothly increases from zero with distance from the bifurcation point. The oscillation frequency in this case does not change noticeably.

Of great interest is the problem of the search for bifurcation points and the frequency of the appearing oscillations in the parameter space of LK equations. The bifurcation points are usually found numerically. The approach to find the bifurcation points, which is based on the linearisation of LK equations near the stationary state, was proposed in paper [5]. The authors managed to reduce the problem to the analysis of two transcendental equations for the frequency of the appearing oscillations, which involve all the physical parameters. This paper shows analytically and numerically that under some conditions the real solutions for the frequency of the field oscillations disappear. The numerical analysis of the behaviour of the roots of the characteristic equation by the contour integral method [3] shows that under these conditions two roots also intersect the imaginary axis, which is a distinctive feature of the Hopf bifurcation. However, the limiting cycle related to the Hopf bifurcation is unstable in this case. As a result, the solution ‘passes away’ to the other stable limiting cycle corresponding to the spike generation regime. The direct calculation of the generation dynamics have shown that this process starts from small harmonic oscillations with the frequency equal to the oscillation frequency at the Hopf bifurcation point and ends by forming periodic anharmonic spikes with a large amplitude. The regime changes with changing the parameters during a large number of oscil-

A.P. Napartovich, A.G. Sukharev State Research Centre of Russian Federation ‘Troitsk Institute for Innovation and Fusion Research’, 142190 Troitsk, Moscow region, Russia, e-mail: napart@mail.ru, sure@triniti.ru

Received 23 November 2007; revision received 8 May 2008
Kvantovaya Elektronika 38 (10) 927–932 (2008)
Translated by I.A. Ulitkin

lations. In the case of the reverse change in the parameters, the stationary regime restores at another point, i.e. a hysteresis takes place. Hard excitation of the spike generation regime, hysteresis during the appearance and disappearance of oscillations and the possibility of controlling the dynamic regimes by fitting the parameters can be of practical interest.

2. Derivation of basic relations

Consider LK equations describing an optical external feedback laser diode in dimensionless variables in the form presented in [6, 7]:

$$\begin{aligned} \frac{\partial E}{\partial t} &= (1 - i\alpha)NE(t) + ME(t - \tau) \exp \left[i \left(\alpha + \frac{\pi}{2} \right) \right], \\ T \frac{\partial N}{\partial t} &= P - N - (1 + 2N)|E|^2. \end{aligned} \quad (1)$$

The first expression describes the behaviour of the field amplitude E in the diode and the second – the population inversion dynamics N . In the derivation of the equations, the time dependence of the field in the form $\exp(-i\omega_0 t)$, where ω_0 is the free-laser frequency, is excluded. In (1), α is the line broadening factor (antiwaveguide parameter); τ is the delay time; α is the phase incursion in the feedback loop after subtraction of $\pi/2$ and the number multiple of 2π : $\alpha + \pi/2 = \omega_0 \tau \pmod{2\pi}$. All the quantities having a time dimension are normalised to the photon lifetime τ_{ph} in the intrinsic resonator of length L : $\tau_{\text{ph}}^{-1} = (c/n)[\alpha_{\text{int}} + (2L)^{-1} \times \ln r^{-1}]$ (c/n is the speed of light in the medium, n is its refractive index, α_{int} are internal losses, r is the reflection coefficient of the crystal facets); for example, $T = \tau_s/\tau_{\text{ph}}$ (τ_s is the carrier lifetime). Other dimensionless variables are: $|E| = (\frac{1}{2}g\tau_s I)^{1/2}$ is the field amplitude (I is the photon density, g is the differential amplification of the medium); $N = \frac{1}{2}g\tau_{\text{ph}}(N_c - N_{\text{th}})$ is the inverse population measured from the threshold population N_{th} (N_c is the carrier concentration); $P = \frac{1}{2}g\tau_{\text{ph}}(j\tau_s - N_{\text{th}})$ is the normalised pump intensity [$j = J/(ed)$ is the carrier injection rate (in $\text{cm}^{-3} \text{s}^{-1}$) into the active layer of thickness d for the current density j , e is the carrier charge]. The coupling constant $M = (1 - r)(R/r)^{1/2} [c\tau_{\text{ph}}(2nL)^{-1}]$, where R is the reflectivity of the external mirror.

The stationary state is determined by the conditions $\partial N/\partial t = 0$, $\partial E/\partial t = i\Omega E$, where Ω is the radiation frequency detuning with respect to ω_0 . These conditions lead to the relations

$$\frac{N}{M} = \sin(\alpha - \Omega\tau), \quad P - N = (1 + 2N)|E|^2.$$

And the frequency detuning Ω satisfies the equation

$$\frac{\Omega\tau}{s} = \sin \left(\Omega\tau - \alpha + \arctan \frac{1}{\alpha} \right). \quad (2)$$

The number of stationary solutions (2) depends of the feedback efficiency [1, 3], which is determined with the accuracy to the multiplier as a product of the coupling constant and the delay time: $s = M\tau(1 + \alpha^2)^{1/2}$. The number of roots in Eqn (2) increases with increasing s . The stability of stationary solutions is determined by the position of roots of the characteristic equation [1, 3]

$$\begin{aligned} g_2(\lambda) &= \lambda(\gamma + \lambda)[1 + M^2 f^2 + 2Mf \sin(\Omega\tau - \alpha)] \\ &+ \left[2 \frac{P + M \sin(\Omega\tau - \alpha)}{T} \right] \left[1 - Mf(1 + \alpha^2)^{1/2} \right. \\ &\left. \times \cos \left(\Omega\tau - \alpha + \arctan \frac{1}{\alpha} \right) \right] = 0 \end{aligned} \quad (3)$$

on the complex plane. Here, the notations $f = [1 - \exp(-\lambda\tau)]/\lambda$ and $\gamma = T^{-1}(1 + 2P)(1 + 2N)^{-1}$ are used for brevity. The stationary state stability is preserved until the number of poles

$$m = 1 + \frac{1}{2\pi i} \int_{+i\infty}^{-i\infty} d\lambda \frac{\dot{g}_2(\lambda)}{g_2(\lambda)} \quad (4)$$

in the right half-plane ($\text{Re} \lambda > 0$) is equal to zero [3]. When the stability of stationary solutions is lost, different oscillations – both periodic and chaotic – appear in the time dependence of the delayed feedback laser power. We will consider the parametric conditions of the appearance of Hopf bifurcations in the solutions of LK equations.

In delayed feedback diode lasers, the frequency ω_r of intrinsic relaxation oscillations is, as a rule, large compared to the inverse lifetime of the carriers: $\omega_r \approx (2P/T)^{1/2} \gg 1/T$. The equations can be linearised near the bifurcation point in small perturbations with respect to the stationary solution. Let us present the field in the form $E = E_{\text{st}} \times \exp \Psi \approx E_{\text{st}}(1 + \Psi)$, where $E_{\text{st}} = [P + M \sin(\Omega\tau - \alpha)]^{1/2} \times \exp(i\Omega t)$. A differential equation with a delayed argument

$$\begin{aligned} -\ddot{\Psi} &= M \exp \left[-i\Omega\tau + i \left(\alpha + \frac{\pi}{2} \right) \right] (\dot{\Psi} - \dot{\Psi}_\tau) \\ &+ (1 - i\alpha)\omega_r^2 \text{Re} \Psi \end{aligned} \quad (5)$$

is derived in [5] for the small complex phase perturbation Ψ . Here, $\Psi_\tau = \Psi(t - \tau)$;

$$\omega_r^2 = 2 \frac{P + M \sin(\Omega\tau - \alpha)}{T}. \quad (6)$$

Because of the delay and a nonanalytic term containing $\text{Re} \Psi$, equation (5) at the Hopf bifurcation point has the solution in the form of a linear combination of two phase-shifted harmonic oscillations: $\Psi = c_1 \cos(\omega t) + c_2 \times \cos[\omega(t - \tau/2)]$, where $c_{1,2}$ are complex numbers. The oscillation frequency ω is found from the existence condition of nontrivial solutions of Eqn (5). By using relations derived in [5] (see also the Appendix), this existence condition is reduced to the analysis of the roots of cubic equation (A4), which can be presented in the form

$$x^3 - px - q = 0, \quad (7)$$

where

$$x = \omega^2 - \Delta; \quad (8)$$

$$\Delta = \frac{2}{3} [\omega_r^2 + 2M^2 \cos^2(\Omega\tau - \alpha)];$$

$$p = 3\Delta^2 - \omega_r^2 \delta; \quad \delta = \omega_r^2 + 4M\Omega \cos(\Omega\tau - \alpha); \quad (9)$$

$$q = 2\Delta^3 - \Delta\omega_r^2 \delta - \omega_r^4 [M^2(1 + \alpha^2) - \Omega^2].$$

The number of real roots of the cubic equation with the real coefficients (7) changes from one to three upon varying the parameter q . As shown in the Appendix, the solution for $\omega^2 > 0$ appears only in the presence of three roots (7). Because the extrema of the function $y = x^3 - px - q$ lies at the points $3x^2 = p$, the three real roots can exist only if $p > 0$. The values of the function y_m in the local extrema is $y_m = \pm 2(p/3)^{3/2} - q$. The number of roots changes when the function touches the abscissa axis, i.e. $y_m = 0$ at this moment. The three real roots exist if only $(q/2)^2 \leq (p/3)^3$. In this case, the solution can be written in the form

$$x_k = 2 \left(\frac{p}{3} \right)^{1/2} \cos \frac{\theta + 2k\pi}{3}, \tag{10}$$

$$\cos \theta = \frac{q}{2} \left(\frac{p}{3} \right)^{-3/2}, \quad k = 0, 1, 2.$$

Among the three roots only one positive root satisfies condition (A3), which guarantees the absence of ‘redundant’ solutions.

Thus, the number of control parameters of the problem can be reduced to two (p, q). The condition

$$q^2 = \frac{4}{27} p^3 \tag{11}$$

divides the regions in the parameter space in which the Hopf bifurcation or bifurcation with a hard excitation of the spike regime are realised. The interface in the parameter space corresponding to this condition can be naturally called separatrix. In terms of the catastrophe theory (see, for example, [8, 9])*, the separatrix is a ‘fold line’ of the cusp catastrophe A_3 .

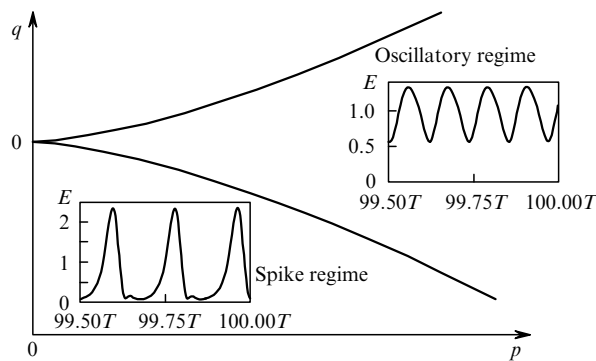


Figure 1. Diagram in the variables p, q illustrating the regions of different nonstationary lasing regimes. The inset shows the characteristic time dependences of the field amplitude E in different regimes.

Thus, under the condition $-(p/3)^{3/2} \leq q/2 \leq (p/3)^{3/2}$, the instability of the stationary state is caused by the Hopf bifurcation. Note that the two roots on the separatrix merge into one multiple root corresponding to the frequency $\omega^2 = \Delta + (p/3)^{1/2}$. In the diagram in variables p, q (Fig. 1) the separatrix separates the region where the instability leads to harmonic oscillations whose amplitude

smoothly increases with deepening into the instability region and the region where the established periodic oscillations are highly anharmonic.

3. Numerical calculations

The numerical program for the solution and analysis of Eqns (1) was developed earlier [3]. It includes the determination of the stationary states followed by the analysis of the stability based on integral calculations (4). The obtained information allows one to select specific values of the phase incursion in the feedback loop \varkappa for calculating the process dynamics. The type of the nonlinear solution (deterministic or chaotic oscillations) is determined by the parallel calculation of the Lyapunov indices and the dimensionality of the phase subspace by the Kaplan–Yorke formula. The direct observation of the generation dynamics near the bifurcation points allows one to determine the bifurcation type. The analytic relations formulated above well agree with the results of the numerical integration. In particular, the oscillation frequency found analytically for the Hopf bifurcation coincides with good accuracy with the result of the direct calculation. In the calculations we used the antiwaveguide parameter $\alpha = 3$.

The establishment of the generation dynamics was calculated as follows: for the specified parameters near the bifurcation point the solution of LK equations was calculated numerically. The established values of the field E and population N in the stationary state are used as initial conditions to make a new calculation with a different \varkappa value. The step for \varkappa was chosen so that to exclude sharp temporal changes in the field after \varkappa is changed.

A classical pattern is observed during the transition through the Hopf bifurcation: within the time of the order of one oscillation time, there appear field oscillations whose amplitude gradually (for the time significantly exceeding the carrier lifetime T) increases to the stationary value. With increasing the distance from the Hopf bifurcation point, the field modulation amplitude increases at an almost constant frequency. The numerical calculations showed that for the pump intensity $P > 0.8$, the coupling constant $M > 0.02$ and the delay time $\tau \geq 40$, the stationary state instability develops according to the Hopf bifurcation scenario.

For the bifurcation with a hard switching on of oscillations, the periodic regime is established for the time exceeding T . First, field amplitude oscillations appear, whose frequency corresponds to the imaginary roots $\lambda = \pm i\omega$ of Eqn (3). Unlike the evolution after the transition through the Hopf bifurcation upon hard switching on of oscillations, their shape during the establishment of the periodic regime changes significantly. In particular, the oscillation period changes. If the current frequency is determined by the oscillation period, the frequency ω varies from 0.049 to 0.035 for the set of parameters $P = 0.8, M = 0.02, T = 1000, \tau = 20, 180^\circ\varkappa/\pi = 225^\circ$. This development dynamics is typical of the instability leading to a transition to the spike regime.

4. Change in the development regime of the oscillatory instability as a function of control parameters

Among a set of physical parameters ($P, M, T, \tau, \varkappa, \alpha$), the line broadening factor α is determined by the laser design

*Note that (7) is a canonical equation for the description of the cusp catastrophe A_3 according to the classification of types of elementary catastrophes presented by Thom.

and, hence, cannot be changed during the experiment. We used in calculations $\alpha = 3$. Because the value of T is high, it was also fixed in calculations and was set equal to 1000. Other parameters (P is the pump intensity, M is the coupling constant, τ is the delay time, κ is the phase incursion of the field in the feedback loop) can be varied in the experiment.

The separatrix corresponding to the change in the scenario of the oscillation development from the stationary state is determined by equality (11) fixing the ratio $27q^2/(4p^3)$, which, as can be shown, depends only on two key parameters: $\beta = \omega_r/M$ and $\chi = \Omega\tau - \kappa$ (χ is the phase of the change in the population, for the stationary state $\sin \chi = -N/M$). It was found numerically that for the interval $1 \leq \omega_r/M \leq 4$ expression (11) has four roots χ_i , each of them depending on ω_r/M . For each branch relations (8), (9) together with expressions (A1) and (A3) from the Appendix allow the calculation of the root of the oscillation frequency at the separatrix points $\omega^2(\beta, \chi) = \Delta + (\Delta^2 - \omega_r^2 \delta/3)^{1/2}$ and the quantity $\omega\tau$. Having determined the delay time τ , by using (2) one can also reconstruct separately Ω and κ – the coordinates of the bifurcation point on the stationary state diagram. Of practical interest is also the function $\tau(P)$ at the separatrix points, which is shown in Fig. 2 for each branch $\chi(\omega_r/M)$ at $\omega_r/M = 2$. The change in the parameters corresponding to the intersection of curves in Fig. 2 is expected to result in the change in the regime of the appearance of oscillations in the unstable stationary state.

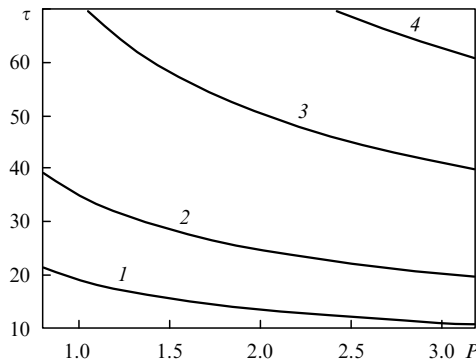


Figure 2. Four separatrices in coordinates τ , P for $\omega_r/M = 2$, $\alpha = 3$, $T = 1000$ corresponding to the solutions $\chi_i(\omega_r/M)$ of equation (11) together with equations (A1)–(A4).

Curve (3) in Fig. 2 corresponds to the case, when the number of roots of dispersion equation (3) in the right half-plane changes from one to three, which is of no practical importance. It was found out that the intersection of curve (4) does not correspond to the intersection of the separatrix in coordinates p , q , which means that the Hopf bifurcation is realised on both sides of the curve.

Thus, only when curves (1) and (2) intersect, the scenario of the development of the stationary state instability is changed. It follows from the above expressions that the oscillation frequency and the delay time in the feedback loop are related, for example, along curve (2) by the relation $\tau = 2.067/\omega$. The quantities $\Omega\tau/s = 0.25$, $\kappa/\pi = 1.38$ and $\chi = 2.56$ are constant along this curve. Figure 3 presents the diagrams of the stationary state stability to illustrate what occurs when curves (1) and (2) intersect.

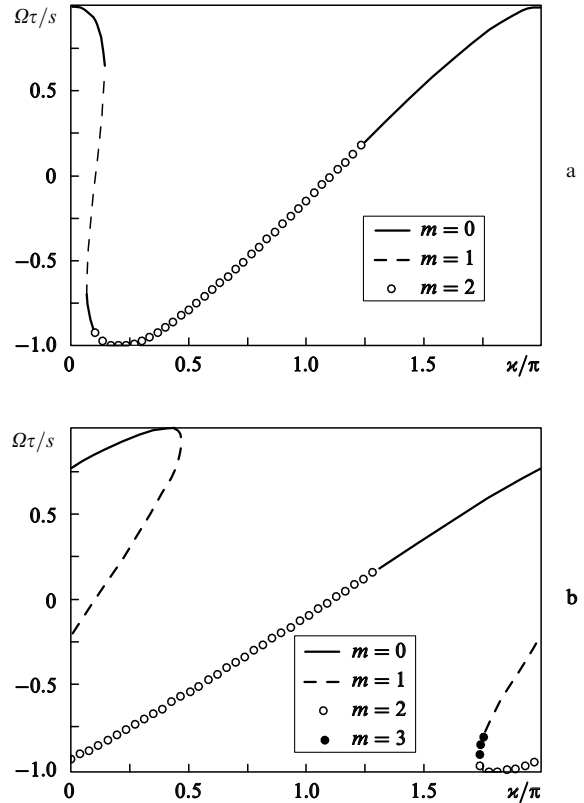


Figure 3. Stability diagrams of the stationary state for $P = 0.8$, $M = 0.02$, $\tau = 20$ (a) and 40 (b) (m is the number of roots for $\text{Re } \lambda > 0$).

They are plotted for the delay time $\tau = 20$ and 40 at fixed $P = 0.8$ and $M = 0.02$.

The plot in Fig. 3a contains two values of κ at which the stationary state stability is violated by the passage of two roots (3) to the right half-plane. One of the bifurcations ($\chi = \pi/12$) is located on the left boundary of the segment with $m = 2$ [the number of roots m in Eqn (3) is determined by using (4)], and the other – on the right boundary of the segment with $m = 2$ and the region with $m = 0$ for the stable stationary state ($\kappa = 5\pi/4$). The first bifurcation turns close to the left edge of separatrix (1) (Fig. 2). Because the stable stationary state adjacent in Fig. 3a with the first bifurcation for $\kappa = \pi/12$ is restricted on the other side by the development of the aperiodic instability for $\kappa = \pi/16$, the interval χ , where it can exist, is very narrow, which is of low interest from the point of view of the experiment. The second bifurcation point in Fig. 3a, as numerical calculations show, corresponds to the hard excitation of the spike regime, whose establishment dynamics is described in the previous section. To change the bifurcation type of this point to the Hopf bifurcation, it is enough to change the delay time τ according to the data for curve (2) in Fig. 2.

The numerical calculations showed that above separatrix (2) (Fig. 2) soft excitation of oscillations occurs, while below it, the hard regime of oscillation excitation is realised. Near the separatrix, when the bifurcation points of both types are close in the parameter space, final states sharply change with varying slightly the physical parameters. One can see from Fig. 2 that for $P = 0.8$, $M = 0.02$, $\tau = 40$ the bifurcation point should be close to separatrix (2). The plot in Fig. 3b shows such a bifurcation point for $180^\circ\kappa/\pi = 235^\circ$ (in this case, $\Omega\tau/s = 0.2$). The Hopf bifurcation is

close to it and harmonic oscillations are established. When \varkappa is changed by one degree to 234° , oscillations develop within the time $\sim 50T$. In this case the current frequency changes from 0.055 to 0.042 and the oscillation shape becomes strongly anharmonic. The transition to the stationary regime from this state upon the reverse change in the parameters occurs for $180^\circ\varkappa/\pi = 252^\circ$, i.e. a hysteresis take place.

Moving along separatrix (2) (Fig. 2), the change in the bifurcation type of creating oscillations can be achieved for a shorter delay time ($\tau = 20$). In this case, P should be set equal to 3.2 (and M – to 0.04, respectively), which also corresponds to the closeness to the separatrix. The Hopf bifurcation is observed for $180^\circ\varkappa/\pi = 229^\circ$ and weak harmonic oscillations with the frequency $\omega = 0.11$ take place in the narrow interval of \varkappa ($229^\circ > 180^\circ\varkappa/\pi > 227^\circ$). At the boundary of the interval for $180^\circ\varkappa/\pi = 227^\circ$, hard switching on of intense oscillations with an almost 100-% field amplitude modulation occurs. The spike regime is changed to the stationary state for $180^\circ\varkappa/\pi = 242^\circ$. According to the stated theory, hard excitation of the spike regime takes place in the entire region below the separatrix and the return to the stationary state is accompanied by the hysteresis.

In the region of the parameters under study, only curve (2) in Fig. 2 is of practical interest for studying the change in the scenarios of the instability development of the stationary generation from the soft to the hard oscillation excitation regimes. The linear stability theory for the conditions of the hard oscillation excitation also predicts a passage of two roots of the characteristic equation to the right half-plane. Numerical and analytical calculations allow one to interpret the found phenomenon as follows. The Andronov–Hopf bifurcation leads to the development of oscillations. The increase in their amplitude is stabilised by the output of the solution to the limiting cycle covering the point of the stationary state. The analysis described above showed that approaching the separatrix, the region of attraction to the limiting cycle narrows down. At the moment of the separatrix intersection, the stability of the limiting cycle is lost. The spike generation regime is the result of the development of the limiting cycle instability.

The operation regimes of a diode laser controlled by a signal with a specified amplitude and frequency were classified in paper [4]. In particular, it was found that the limiting cycle created by the Hopf bifurcation can experience the saddle–node bifurcation with a transition to a new limiting cycle. The interaction of limiting cycles is a nonlinear process. By using the linear theory we managed to find the parameters of the problem for which the established nonlinear generation regime is changed.

Our interpretation of the processes is also supported by the hysteresis observed in the spike generation regimes: the return to the stationary regime by means of the reverse change in the parameters takes place at other values of these parameters, so that two stable generation regimes – the stationary and dynamic spike regime – exist for the same parameters in the overlap region.

Thus, separatrix (2) (Fig. 2) is most interesting for classifying the nonlinear lasing regimes. In the space of three parameters (τ , P , M), the searched for separatrix can be plotted in the form of the function $\tau(P, M)$ representing a surface in a three-dimensional space. The relief of this function resembles a slope of a hill with a maximum in

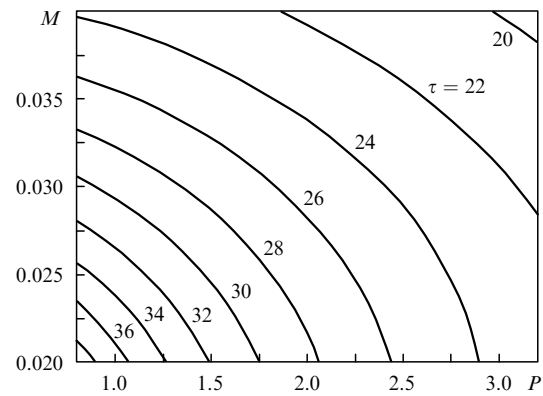


Figure 4. Representation of separatrix (2) in Fig. 2 in the form of equal level lines of the function $\tau(P, M)$.

the left bottom part of the domain of definition (Fig. 4). The surface relief is presented in the form of the level lines. Curve (2) in Fig. 2 is the intersection of the surface $\tau(P, M)$ with the surface corresponding to $\omega_r/M = 2$ and passes through the left bottom and right top parts of the definition domains.

For the specified parameters τ , P , M , by fitting the field phase incursion \varkappa in the feedback loop, the regime of small harmonic oscillations or periodic nonharmonic spikes can be provided (the jump $m = 0 \rightarrow 2$ in Fig. 3). Above the separatrix surface $\tau(P, M)$ the Hopf bifurcation is realised, which leads to small oscillations and below the separatrix hard excitation of oscillations occurs. In the general case, the normal vector $\{-\delta\tau/\delta P, -\delta\tau/\delta M, 1\}$ to the surface $\tau(P, M)$ in the three-dimensional space $PM\tau$ directs the change in the parameters to the scenario with a soft excitation of oscillations.

Therefore, to pass from the regime of small oscillations to the spike generation regime it is necessary to decrease the round-trip time of radiation in the feedback loop by adjusting the pump power in this case. In particular, if M is fixed and P decreases, the bifurcation type of creating oscillations changes from the Hopf bifurcation to the hard excitation regime of oscillations. Thus, for $\tau = 30$ and $M = 0.02$ the Hopf bifurcation is possible if $P(M) > 1.75$. For the fixed P the change of the Hopf bifurcation to the hard excitation regime of oscillations occurs if the coupling constant M is decreased.

5. Conclusions

Our analysis has shown the existence of the parameter space of a delayed feedback diode laser in which small oscillations of a generated field appearing due to the Hopf bifurcation become unstable and transform into spikes with a new repetition rate. Within the framework of the linear theory with respect to the closeness to the bifurcation point, the algebraic equation is derived from which the real oscillation frequency can be found. It has been found that although the oscillatory instability remains, the solution of the algebraic equation yielding the oscillation frequency vanishes under certain conditions. This behaviour of the system can be interpreted as a change in the scenario of the instability development. Numerical calculations have shown that during the transition through the point in the parameter space in which the oscillation frequency obtained

from the algebraic equation disappears, the character of oscillation excitation drastically changes. Small oscillations typical of the Hopf bifurcation are transformed for the time exceeding the carrier relaxation time into periodic oscillations of the finite amplitude, whose shape resembles spikes. In other words, for the arbitrary small change in the parameters leading to the instability region, the amplitude of the established oscillations turns to be finite and their shape noticeably differs from the harmonic one.

The performed analysis has allowed five initial physical parameters, on which lasing depends, to be reduced to only two their combinations. We have derived a simple equation determining the parameters at which there occurs the change in the regime of the instability development of the stationary lasing having a character of the phase transition. The relation of the performed analysis to the catastrophe theory has been pointed out. In particular, the separatrix separating different regimes of the instability development in the parameter space is a 'fold line' on the cusp surface in the terms of the catastrophe theory. It has been found in numerical calculations that the more the time of the establishment of the stationary oscillations the closer the system to the critical point. It has been also determined that when the oscillation excitation is step-wise, there exists the hysteresis of the lasing dynamics. In the hysteresis region lasing depends on the prehistory.

From the practical point of view the performed analysis is useful for the controlled change in the lasing dynamics of a delayed feedback diode laser. The presented theory allows the selection of physical parameters to obtain lasing in the regime of generation of short pulses. The parameter space where this regime is realised is wider for lasers with a small delay time of the field in the feedback loop. At a high pump level the modulation depth almost achieves 100%. Harmonic oscillations appearing during the Hopf bifurcation are better realised in lasers with longer delay times in the feedback loop.

Appendix

It was shown in [5] that the nontrivial solution of equation (5) exists if the frequency ω satisfies the system of two transcendent equations

$$\omega^2 = \omega_r^2 + 4M^2 \sin^2 \frac{\omega\tau}{2}, \quad (\text{A1})$$

$$M\omega \sin(\omega\tau) = \frac{1}{2} \omega_r^2 (1 + \alpha^2)^{1/2} \sin(\Omega\tau - \varkappa - \arctan \alpha) - \omega^2 \sin(\Omega\tau - \varkappa). \quad (\text{A2})$$

Under condition that

$$M\omega \sin(\omega\tau) \left[\frac{1}{2} \omega_r^2 (1 + \alpha^2)^{1/2} \sin(\Omega\tau - \varkappa - \arctan \alpha) - \omega^2 \sin(\Omega\tau - \varkappa) \right] \geq 0, \quad (\text{A3})$$

system of equations (A1), (A2) is equivalent to the bicubic equation:

$$\omega^2(\omega^2 - \omega_r^2)(4M^2 + \omega_r^2 - \omega^2)$$

$$= 4M^2 \left[\frac{1}{2} \omega_r^2 (1 + \alpha^2)^{1/2} \sin(\Omega\tau - \varkappa - \arctan \alpha) - \omega^2 \sin(\Omega\tau - \varkappa) \right]^2. \quad (\text{A4})$$

One can conclude from the form of the left-hand side of Eqn (A4) that one of its roots is always negative (Fig. A1). Thus, this root does not correspond to the Hopf bifurcation. The cubic equation can have either one or three real roots. Only in the latter case we can expect the appearance of real oscillation frequencies (i.e. roots for $\omega^2 > 0$). Therefore, it is necessary that all the three roots of the cubic equation are real for the Hopf bifurcation to appear.

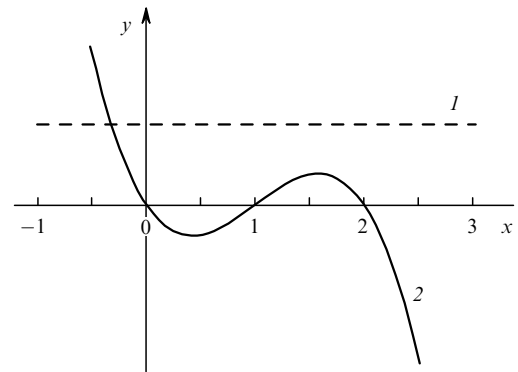


Figure A1. Illustration to the solution of equation (A4): $y = \text{const} > 0$ (l), $y = x(x - x_1)(x_2 - x)$, $x = \omega^2$, $x_1 = \omega_r^2$, $x_2 = \omega_r^2 + 4M^2$ (2).

References

1. Verduyn Lunel S.M., Krauskopf B., in *Fundamental Issues of Nonlinear Laser Dynamics*. Ed. by B. Krauskopf, D. Lenstra (Melville, NY: AIP Conf. Proc., 2000) Vol. 548, p.66.
2. Lang R., Kobayashi K. *IEEE J. Quantum Electron.*, **16**, 347 (1980).
3. Napartovich A.P., Sukharev A.G. *Kvantovaya Elektron.*, **34** (7), 630 (2004) [*Quantum Electron.*, **34** (7), 630 (2004)].
4. Wiecezorek S., Krauskopf B., Lenstra D. *Opt. Commun.*, **172**, 279 (1999).
5. Sukharev A.G., Napartovich A.P. *Kvantovaya Elektron.*, **37** (2), 149 (2007) [*Quantum Electron.*, **37** (2), 149 (2007)].
6. Winful H.G., Rahman L. *Phys. Rev. Lett.*, **65** (13), 1575 (1990).
7. Winful H.G., Wang S.S. *Appl. Phys. Lett.*, **53** (20), 1894 (1988).
8. Gilmore R. *Catastrophe Theory for Scientists and Engineers* (New York: Wiley, 1981; Moscow: Mir, 1984).
9. Arnold V.I. *Usp. Matem. Nauk*, **30** (5), 3 (1975).